BOUNDS ON THE CABIBBO–KOBAYASHI–MASKAWA MATRIX ELEMENTS $|V_{td}|$ AND $|V_{ts}|$ FROM EXPERIMENTS ON $B^0-\bar{B}^0$ MIXINGS

A. ALI
Deutsches Elektronen Synchrotron, DESY, D-2000 Hamburg, Fed. Rep. Germany

B. VAN EIJK [1] and I. TEN HAVE [1]
NIKHEF, 1009 DB Amsterdam, The Netherlands

Received 2 February 1987

We present a theoretical analysis of the process $p\bar{p} \to \mu^\pm X$, $\mu^\pm\mu^\pm X'$, $\mu^+\mu^- X'$ due to heavy flavour production and decays, based on perturbative quantum chromodynamics, QCD. We find reasonable agreement for the inclusive rates and distributions between the UA1 measurement and our calculations, with the exception of the dimuon ratio $R(\pm\pm/+-)$, which is found typically a factor ~1.8 smaller than the UA1 data. We interpret this excess in terms of $B_s^0-\bar{B}_s^0$ mixing and obtain a lower bound on the mixing probability, $r_s > 0.14$. In the standard model this implies a lower bound on the Cabibbo–Kobayashi–Maskawa matrix element $|V_{ts}|$ given the top quark mass. The lower bound on $|V_{ts}|$ and the upper bound on $|V_{td}|$, obtained from the (upper bound) $B_d^0 - \bar{B}_d^0$ mixing probability, r_d, from e^+e^- experiments are worked out.

1. Introduction. We address the question of heavy flavour (charm, bottom and top) production at the CERN Sp$\bar{p}$S collider, in the context of perturbative quantum chromodynamics, QCD, concentrating on the inclusive muon and dimuon data measured by the UA1 Collaboration [1]. Our first aim in this paper is to show that QCD calculations quantitatively account for the large p_t and/or central production of heavy flavours at CERN collider energies. This observation is in direct contrast with similar attempts at lower ISR–FNAL energies, which have failed to reproduce the data on charm hadron production [2]. We present here the essential features of a detailed theoretical analysis that we have recently finished [3] for the inclusive muon and the so-called non-isolated dimuon data in the process $p\bar{p} \to \mu^\pm X$, $\mu^\pm\mu^\pm X'$, $\mu^+\mu^- X'$. The corresponding isolated $\mu^+\mu^- X$ data are already well understood in terms of Drell–Yan processes in QCD [4].

Our second aim is to estimate the dimuon ratio $R(\pm\pm/+-)$ in $p\bar{p}$ collisions and compare it, under identical acceptance conditions, with the corresponding UA1 ratio. As we are going to show below, we find $R(\pm\pm/+-) = 0.24 \pm 0.05$. The theoretical error here reflects the various experimental uncertainties on the input parameters concerning heavy flavour production and decays. Compared with the UA1 measurement $R(\pm\pm/+-) = 0.42 \pm 0.07 \pm 0.03$, our estimates are typically a factor ~1.8(2.4σ) below the data. We take the experimental excess seriously and follow up its earlier interpretation [5] in terms of $B^0-\bar{B}^0$ mixing [6], getting bounds on the quantity χ where $\chi \equiv \Gamma(B \to \ell^+ X)/\Gamma(B \to \ell^\pm X)$. The estimate of χ from UA1 data is, within 1σ, consistent with the upper bounds obtained in e^+e^- continuum experiments [7], namely $\chi < 0.12$ (90% CL). The corresponding bound on the quantity $\chi_d \equiv \Gamma(B_d \to \ell^+ X)/\Gamma(B_{\underline{d}} \to \ell^\pm X)$ obtained from the process $e^+e^- \to \Upsilon \to B_d\bar{B}_d, B_u\bar{B}_u$, by the ARGUS collaboration at DORIS, namely $\chi_d < 0.11$ (90% CL) [8], allows significant mixing in the $B_s^0-\bar{B}_s^0$ sector only. We determine the lower bound on the $B_s^0-\bar{B}_s^0$ mixing measure r_s, $r_s \equiv \chi_s/(1-\chi_s)$, from the UA1 data. In the standard three family model, the lower bound on r_s and the upper bound on r_d from the two experiments are equivalent to a lower bound on the Cabibbo–Kobayashi–Maskawa [9]

[1] Also at CERN, CH-1211 Geneva 23, Switzerland.

(CKM) matrix element $|V_{ts}|$ and an upper bound on $|V_{td}|$, respectively, given the top quark mass m_t. Our third aim is to determine these bounds as function of m_t. We will take up these points one by one.

2. Heavy flavour production at the CERN collider. As we have stated at the very outset, the calculations for the heavy flavour production presented here are performed in the framework of perturbative QCD. We have taken into account the following three processes [‡1]:

(a) $p\bar{p} \to QX\ (Q = c, b, t)$

(b) $p\bar{p} \to W^{\pm}X \to cs, tbX'$

(c) $p\bar{p} \to Z^0X \to c\bar{c}, b\bar{b}, t\bar{t}X'$

where all the $2 \to 2$ and $2 \to 3$ processes at the Born level are taken into account. For example, for the class (a) the lowest order fusion process [10] leading to heavy quark–antiquark pair production

$$q\bar{q} \to Q\bar{Q}\,, \quad gg \to Q\bar{Q} \tag{1}$$

and the three processes, contributing to inclusive heavy flavour production in $O(\alpha_s^3)$ [11],

$$q\bar{q} \to Q\bar{Q}g\,, \quad gg \to Q\bar{Q}g\,, \quad gq \to Q\bar{Q}q \tag{2}$$

are included in our estimates of the heavy flavour cross-sections, which we shall be calling QCD contributions. The calculations for the processes (b) and (c) include up to $O(\alpha_s)$ terms [12]. In all processes (a)–(c), quark masses are taken into account in the relevant matrix elements.

It is well known that the processes (a)–(c) are finite in the lowest order. For the processes (1), m_Q regulates the infra-red divergence. Inclusion of the processes (2), for example, leads to both infra-red ($E_i \to 0, i = q, g$) and collinear divergences ($\theta_{ij} \to 0$, with i an initial parton and j a light quark or gluon). The removal of these divergences necessarily requires a complete calculation to order α_s^3, thus needing the virtual corrections to the process (1). This we do not have at hand. Instead, we have put a cut-off on the transverse momentum, p_t^{cut}, of the light quark and gluon by requiring $p_t^{q,g} > p_t^{cut}$ and use $p_t^{cut} = 5$ GeV/c as a reasonable value for all the processes (a)–(c) reported here. This procedure removes all the divergencies and the remaining contributions are genuine hard collisions. The price that one has to pay for such a procedure is that the theoretical cross sections (a)–(c) become p_t^{cut} dependent. However, in a genuine higher order calculation one expects, after the divergencies have been properly regulated, that this dependence would be mild. For example, it has been shown [13] that for the process $gq \to Q\bar{Q}q$ the quadratic divergencies cancel, the logarithmic divergencies can be absorbed in the incoming hadron wave functions. In the remaining cross sections, all propagators are off-shell by at least $\sim m_Q^2$. Likewise, final state quadratic divergencies are guaranteed to cancel and the remaining cross section should show a logarithmic dependence on resolution parameters, for example in ϵ, δ, a la Sterman–Weinberg [14]. These logarithmic terms can be exponentiated in an analogous way as has been done for the p_t^W calculations in order α_s [12]. The point we are driving here is that after incorporating any reasonable smoothing procedure, the cross section below p_t^{cut} must not be a large number for heavy flavour production processes (a)–(c). Our choice here amounts to assuming $\sigma(p_t < p_t^{cut}) = 0$ for $2 \to 3$ processes, and neglecting virtual corrections to $2 \to 2$ processes. Thus our calculations are subject to finite renormalization corrections, which, however, we expect to be small.

Having stated our theoretical framework we proceed to define the various inputs that we have used to arrive at the final expressions. We make use of the EHLQ structure functions [15] with the QCD parameter $\Lambda = 0.2$ GeV and set the Q^2 scale $Q^2 = p_t^2 + m_Q^2$; for the heavy quark masses we use $m_c = 1.75$ GeV/c^2, $m_b = 5.1$ GeV/c^2 and two values for the top quark mass: $m_t = 23, 40$ GeV/c^2. Since we shall be analysing data on centrally produced muons and dimuons, which by the trigger conditions have substantial p_t, the observed muon and dimuon cross sections are not very sensitive on the precise values of m_c and m_b. The choice $Q^2 = p_t^2 + m_Q^2$ is motivated by a recent analysis of the UA1 jet data [16].

To incorporate the fragmentation of heavy quarks we use the parametrization as given by Peterson et al. [17], defined as

‡1 For convenience we denote $W^{\pm} \to \bar{q}q', q\bar{q}'$ by $W^{\pm} \to qq'$ throughout the paper.

$$f(z)=\frac{z(1-z)^2}{[z(1-z)-(1-z)-\epsilon_Q z]^2}\,, \qquad (3)$$

with z being the light-cone variable, $z = (E+p_\parallel)^H/(E+p_\parallel)^Q$. We have used the analysis of Bethke [18] for the extraction of ϵ_c from e^+e^- data, which gives $\epsilon_c = 0.05$ leading to the average value $\langle z_c\rangle = 0.68$, after correcting for the leading order QCD and QED effects. The corresponding numbers for bottom and top quark fragmentation parameters used in our analysis are as follows

$$\epsilon_b = 0.015\,, \quad \langle z_b\rangle = 0.77\,,$$

$$\epsilon_t = 0.0002\,, \quad \langle z_t\rangle = 0.93\,. \qquad (4)$$

The value of ϵ_b is in agreement with e^+e^- data and ϵ_t is our extrapolation.

We have implemented all the known weak decays of charm and bottom hadrons experimentally known so far. The normalizations and shapes of all lepton and hadron energy distributions have been checked against the available data; the details of these comparisons are given in ref. [3]. For the top quark decays we have used the V–A decay matrix elements, as expected in the standard model, and have assumed that the dominant decays of the top quark are given by the final states [19]:

$$t\to b u\bar{d}\,,\quad t\to b c\bar{s}\,,\quad t\to b\ell^+\nu_\ell\quad (\ell = e,\mu,\tau). \qquad (5)$$

The complete cascade $t\to b\to c\to s$ is developed, using the b and c decays as discussed earlier.

Finally, in comparing with the UA1 data we have put in all the acceptance corrections in vogue. We emphasize that the complete development of the hard scattering process in terms of observed hadrons, leptons and photons is implemented in the form of an event generator. The calculations reported here are part of a QCD based multi-purpose Monte Carlo program for proton–antiproton (proton) collisions at high energies, called EUROJET [20].

In table 1 we present the inclusive heavy quark cross sections for the QCD processes (a) and for the exclusive final states involving at least one heavy quark from $W^\pm$ and Z^0 production processes (b) and (c). The cross sections presented are the sum of the leading order $2\to 2$ and $2\to 3$ processes discussed earlier. In the case of charm quark production from QCD processes we have put an additional cut on $\sqrt{\hat{s}}$, namely $\sqrt{\hat{s}} > 10$ GeV for $2\to 2$ and $\sqrt{\hat{s}} > 15$ GeV for $2\to 3$. This, however has no effect on the inclusive muon cross sections. Removing the cut increases the inclusive charm cross section to ~180 μb. Particularly interesting for the ratio $R(\pm\pm/+-)$ is the inclusive bottom cross section at $\sqrt{s} = 630$ GeV, which we es-

Table 1
The heavy quark inclusive cross sections in the processes $p\bar{p}\to QX$ (Q = c, b, t) from the QCD and weak production ($W^\pm$, Z^0) summed over the leading and next to leading orders in α_s at $\sqrt{s} = 630$ GeV. For $2\to 3$ processes we have used a cut-off $p_t^{cut} = 5$ GeV/c. In addition, QCD contributions are calculated with $\sqrt{\hat{s}} > 10$, 15 GeV for $2\to 2$ and $2\to 3$ processes, respectively.

QCD processes	Weak process	Cross section (nb)
$c\bar{c}$		120000
$b\bar{b}$		19000
$t\bar{t}$ (m_t = 23 GeV/c^2)		52
$t\bar{t}$ (m_t = 40 GeV/c^2)		2.2
	$W^\pm\to cs$	1.7
	$W^\pm\to tb$ (m_t = 23 GeV/c^2)	1.5
	$W^\pm\to tb$ (m_t = 40 GeV/c^2)	1.1
	$Z^0\to c\bar{c}$	0.42
	$Z^0\to b\bar{b}$	0.52
	$Z^0\to t\bar{t}$ (m_t = 23 GeV/c^2)	0.31
	$Z^0\to t\bar{t}$ (m_t = 40 GeV/c^2)	0.086

timate to be O(20 μb). Even for large p_t^b and central production we find that the bottom quark cross section is very sizeable at CERN Sp$\bar{p}$S collider energies. For example, for $|p_t^b| > 5$ GeV/c and $|\eta^b| < 2.0$ we find $\sigma(p\bar{p} \to bX) \sim 2$ μb. In comparison, the inclusive top cross section is rather modest, we estimate $\sigma(p\bar{p} \to tX) \sim 3.6$ nb for $m_t = 40$ GeV/c, the larger fraction of which is due to QCD production process (a).

3. The ratio R(±±/+−). The inclusive muon, dimuon and trimuon cross sections from the processes (a)–(c) at $\sqrt{s} = 630$ GeV are given in table 2. The cross sections for the three final states involving muons are calculated for different triggers, with the specific choice in each case motivated by the UA1 analysis. We note that the inclusive muon cross section is almost equally contributed to by the charm and bottom quark. The dimuon cross section is dominated by the b$\bar{b}$ contribution, which constitutes >75% of the inclusive dimuon cross section, for example for $m_t \geqslant 40$ GeV/c^2. The dimuon ratio $R(\pm\pm/+-)$ depends on the relative contribution of the c$\bar{c}$ state (which gives rise to $\mu^+\mu^-$X events only) and the t$\bar{t}$ cross sections (which give intrinsically large values for the ratio $R(\pm\pm/+-)$). The contribution of the top quark to the cross section, however, is bounded from above due to the experimental lower bound on m_t [21]. For the two choices $m_t = 23$ GeV/c^2 and $m_t = 40$ GeV/c^2, the results are given in table 3. We see that the data on $R(\pm\pm/+-)$ prefers a lower value of m_t! The error due to the charm quark contribution is a result of non-trivial input parameters, m_c, ϵ_c, D*/D ratio, m_s, and the experimental errors on the

Table 3
Estimates of the ratio $R(\pm\pm/+-)$ in the process $p\bar{p} \to \mu^\pm\mu^\pm X$, $\mu^+\mu^-X$ with the dimuon cuts stated in table 2 assuming 15% cc contribution to the dimuon cross section [1].

m_t (GeV/c^2)	x_s	P_s	$R(\pm\pm/+-)$
23	0	0.16	0 23
40	0	0.16	0.20
40	0.5	0.16	0.35
40	0.5	0.20	0.38

Table 2
Inclusive muon, dimuon and trimuon cross sections from the processes (a)–(c) calculated at $\sqrt{s} = 630$ GeV, with the following acceptance cuts.
(i) Inclusive – $\mu^\pm$. $p_t^\mu \geqslant 3.0$ GeV/c, $|\eta^\mu| < 1.5$,
(ii) Inclusive – $\mu^\pm\mu^\pm$, $\mu^+\mu^-$ $p_t^{\mu_1,\mu_2} \geqslant 3.0$ GeV/c, $|\eta^{\mu_1}| < 1.3$, $|\eta^{\mu_2}| < 2.0$ and $M^{\mu\mu} > 6$ GeV/c^2,
(iii) Inclusive – 3μ: $p_t^{\mu_i} \geqslant 3.0$ GeV/c, $|\eta^{\mu_i}| < 2.0, i = 1, 2, 3$.

QCD processes	Weak processes	Cross sections (pb)			
		$\sigma(\mu^\pm X)$	$\sigma(\mu^+\mu^- X')$	$\sigma(\mu^\pm\mu^\pm X')$	$\sigma(3\mu X'')$
c$\bar{c}$		160 000	1300	–	–
b$\bar{b}$		180 000	3600	850	89
t$\bar{t}$ (m_t = 23 GeV/c^2)		6100	660	310	78
t$\bar{t}$ (m_t = 40 GeV/c^2)		390	60	33	12
	$W^\pm \to$ cs	84	–	–	–
	$W^\pm \to$ tb (m_t = 23 GeV/c^2)	340	26	27	5.6
	$W^\pm \to$ tb (m_t = 40 GeV/c^2)	270	24	21	4.6
	$Z^0 \to$ c$\bar{c}$	22	1.5	–	–
	$Z^0 \to$ b$\bar{b}$	57	4.4	3.1	0.71
	$Z^0 \to$ t$\bar{t}$ (m_t = 23 GeV/c^2)	47	5.6	3.9	1.2
	$Z^0 \to$ t$\bar{t}$ (m_t = 40 GeV/c^2)	15	22	1.2	0.38

semileptonic branching ratios. Taking all the errors into account we estimate

$$R(\pm\pm/+-) = 0.24 \pm 0.05 \,. \qquad (6)$$

This number is to be compared with the UA1 result [1]

$$R(\pm\pm/+-) = 0.42 \pm 0.07 \pm 0.03 \,. \qquad (7)$$

When we add the statistical and systematical errors in quadrature we find that (7) is typically a factor ~1.8 (2.4 σ) too large.

Apart from the dimuon ratio $R(\pm\pm/+-)$ the inclusive muon and dimuon cross sections as well as various other distributions in p_t^{μ}, the invariant dimuon mass $M^{\mu\mu}$, $p_t^{\mu\mu}$, the azimuthal angle distribution $\Delta\phi^{\mu\mu}$ of the UA1 data are well explained by the

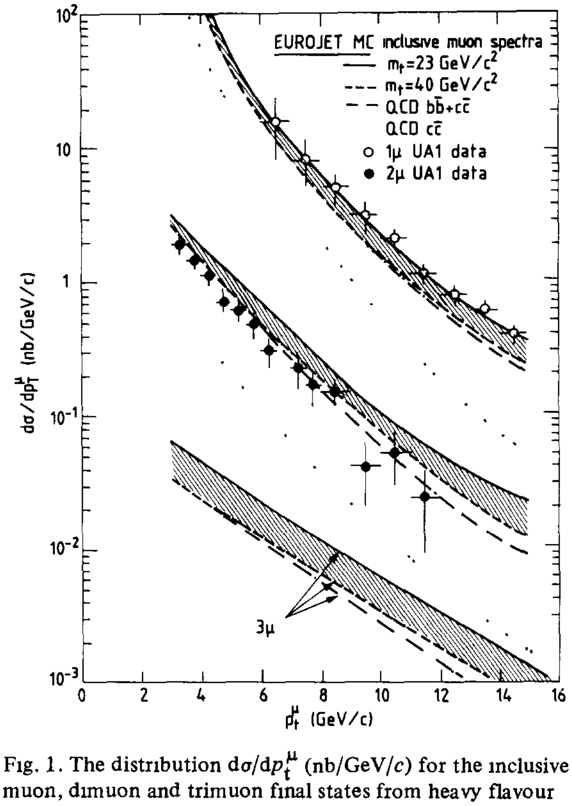

Fig. 1. The distribution $d\sigma/dp_t^{\mu}$ (nb/GeV/c) for the inclusive muon, dimuon and trimuon final states from heavy flavour production processes (a)–(c), at the CERN Sp$\bar{p}$S collider at $\sqrt{s}$ = 630 GeV. The data points are from UA1 [1]. The distributions satisfy the following acceptance cuts: (i) inclusive – $\mu^{\pm}$. $p_t^{\mu} \geq 3.0$ GeV/c, $|\eta^{\mu}| < 1.5$, (ii) inclusive – $\mu^{\pm}\mu^{\pm}$, $\mu^{+}\mu^{-}$ $p_t^{\mu_1,\mu_2} \geq 3.0$ GeV/c, $|\eta^{\mu_1}| < 1.3$, $|\eta^{\mu_2}| < 2.0$ and $M^{\mu\mu} > 6$ GeV/c^2 (so-called non-isolated dimuons only), (iii) inclusive – 3μ: $p_t^{\mu_i} \geq 3.0$ GeV/c, $|\eta^{\mu_i}| < 2.0, i = 1,2,3$.

QCD calculations presented here. Leaving detailed comparisons of other distributions to ref. [3], we show in fig. 1 the p_t^{μ} distributions for the processes $p\bar{p} \to (\mu, 2\mu, 3\mu)\,X$ and compare them with the available data. We note that the overall normalizations and shapes are reasonably well reproduced, confirming that heavy flavour production at collider energies is under the quantitative control of perturbative QCD. As we have noted earlier, the dimuon final state is dominated by the bb contribution and, very probably, the resolution of the discrepancy between the estimates (6) and the measurements (7) has to be sought in the bottom sector. We discuss this point in the next section.

4. B^0–$\bar{B}^0$ oscillations and bounds on $|V_{td}|$ and $|V_{ts}|$. The scenario and detailed calculations of B^0–$\bar{B}^0$ oscillations are well documented in the literature [22,19]. We recall that there are two neutral bottom mesons B_d^0 ($\equiv \bar{b}d$) and B_s^0 ($\equiv \bar{b}s$) which are mixed with their charge conjugates $\bar{B}_d^0$ and $\bar{B}_s^0$, respectively. The implication of such mixings in the present context is obvious. The ratio $R(\pm\pm/+-)$ would be enhanced thus bringing theoretical estimates and the UA1 data closer to each other. To quantify this agreement we define the mixing probabilities r_d and r_s ($0.0 \leq r_{d,s} \leq 1.0$) by the well-known ratio [23]

$$r_q \equiv \frac{\Gamma(B_q \to \ell^+ X)}{\Gamma(B_q \to \ell^- X)}, \quad q = d, s \,, \qquad (8)$$

which can be expressed in terms of the normalized mass and width differences x_q and y_q ($x_q = (\Delta M/\Gamma)_q$, $y_q = (\Delta\Gamma/2\Gamma)$, $\Gamma = (\Gamma_H + \Gamma_L)/2$)

$$r_q = \frac{x_q^2 + y_q^2}{2 + x_q^2 - y_q^2} \sim \frac{x_q^2}{2 + x_q^2} \to 1 |_{x_q \gg 1} \,. \qquad (9)$$

The second relation follows from theoretical calculations which predict $y_q^2/x_q^2 \ll 1$ for both B_d^0–$\bar{B}_d^0$ and B_s^0–$\bar{B}_s^0$ mixing [22,19]. In the analysis of experimental data it is often useful to define a related quantity, χ_q,

$$\chi_q = \frac{\Gamma(B_q \to \ell^+ X)}{\Gamma(B_q \to \ell^{\pm} X)} = \frac{r_q}{1 + r_q} \,. \qquad (10)$$

The quantity used by the experimental groups at CESR and DORIS Y_d, is simply expressed as

$$Y_d = \frac{N(B_d^0 B_d^0) + N(\bar{B}_d^0 \bar{B}_d^0)}{N(B_d^0 \bar{B}_d^0)} = \frac{\chi_d}{1 - \chi_d}, \qquad (11)$$

and the ratio $R(\pm\pm/+-)$, for measurements in the continuum experiments, for example at PEP, PETRA and the CERN collider, is given by

$$R(\pm\pm/+-) = \frac{2\chi(1-\chi)}{\chi^2 + (1-\chi)^2} \underset{\chi \ll 1}{\sim} \frac{2\chi}{1-\chi}, \qquad (12)$$

where χ is the weighted average of χ_d and χ_s defined above

$$\chi = [(BR)_d P_d \chi_d + (BR)_s P_s \chi_s]/\langle BR \rangle . \qquad (13)$$

P_d (P_s) is the probability that a b quark will end up in a B_d^0 (B_s^0) meson; $(BR)_d$ [$(BR)_s$] is the semileptonic branching ratio for the B_d^0 (B_s^0) meson and $\langle BR \rangle$ is the average semileptonic branching ratio for the bottom hadrons. There are good theoretical reasons to assume that the semileptonic branching ratios and the lifetime of the bottom hadrons B_d^0, $B_u^\pm$, B_s^0, Λ_b^0 are very similar [24]. This simplifies the expression (13)

$$\chi = P_d \chi_d + P_s \chi_s . \qquad (14)$$

The quantities P_d and P_s have to be determined from experiments. As a first approximation we assume that P_d (P_s) is given by the probability of exciting a $d\bar{d}$($s\bar{s}$) pair from the vacuum, at a given energy. This would suggest $P_d \sim 0.35$–0.40 and $P_s \sim 0.15$–0.20, expected from measurements in e^+e^- and hadronic collisions. The intrinsic mixing parameters χ_d and χ_s need evaluation of the mass difference ratios x_d and x_s. It is generally expected that due to the large bottom quark mass, $m_b \sim 5$ GeV/c^2, the quantities x_d and x_s are dominated by the short-distance piece. Thus, x_d, x_s can be calculated by the box diagram contribution, giving

$$x_d = \left(\frac{\Delta M}{\Gamma}\right)_d = \frac{G_F^2 f_{B_d}^2 m_{B_d}}{6\pi^2 \Gamma_d} M_W^2 \mathcal{B} F_d(m_b, m_t, \lambda),$$

$$x_s = \left(\frac{\Delta M}{\Gamma}\right)_s = \frac{G_F^2 f_{B_s}^2 m_{B_s}}{6\pi^2 \Gamma_s} M_W^2 \mathcal{B} F_s(m_b, m_t, \lambda), \qquad (15)$$

where f_{B_d} (f_{B_s}) is the B_d^0 (B_s^0) pseudoscalar meson coupling constant and $\mathcal{B}$ is the so-called bag constant, expected to be close to 1 for bottom hadrons. The functions $F_{d,s}(m_b, m_t, \lambda)$ depend on quark masses and the CKM matrix elements, and are dominated by the top quark contribution.

$$F_d(m_b, m_t, \lambda) \sim U_t |\lambda_{td}|^2 ,$$

$$F_s(m_b, m_t, \lambda) \sim U_t |\lambda_{ts}|^2 . \qquad (16)$$

To a very good approximation the quark mass functions U_t can be expressed as [25] (see also ref. [22])

$$U_t \sim m_t^2 / M_W^2 \eta^B + O(m_b^2/m_t^2) \qquad (17)$$

where η^B is a QCD correction factor estimated to lie in the range $0.81 \leqslant \eta^B \leqslant 0.86$ for $25 \leqslant m_t \leqslant 60$ GeV/c^2 and $0.1 \leqslant \Lambda_{MS} < 0.2$ GeV. The CKM factors $\lambda_{td,ts}$ are given by

$$|\lambda_{td}| = |V_{tb}^* V_{td}|, \quad |\lambda_{ts}| = |V_{tb}^* V_{ts}| . \qquad (18)$$

Our approach is to determine χ from the UA1 data on $R(\pm\pm/+-)$ and use the upper bound on χ_d from ARGUS to set a lower limit on χ_s (equivalently r_s). These bounds will in turn be used to set corresponding bounds on the CKM matrix angles $|V_{td}|$ and $|V_{ts}|$ as functions of m_t. The values that we have used for the various constants appearing in (15) are as follows

$$\Gamma_d = \Gamma_s = h/\langle\tau_B\rangle = (5.93^{+0.86}_{-0.66}) \times 10^{-13}\ \text{GeV},$$

$$\mathcal{B} f_{B_d}^2 = (0.11\ \text{GeV})^2, \quad \mathcal{B} f_{B_s}^2 = (0.15\ \text{GeV})^2, \qquad (19)$$

where we have used the present world average of the bottom lifetime [26] $\tau_B = (1.11 \pm 0.14) \times 10^{-12}$ s and the recent calculations of the coupling constants in the QCD sum rule approach [24], which generally is found to be in reasonable agreement with data. To get an idea of the values for x_d and x_s in the standard model, a good estimate is

$$x_d = 0.05 \left(\frac{m_t}{40\ \text{GeV}/c^2}\right)^2 \frac{\mathcal{B} f_{B_d}^2}{(110\ \text{MeV})^2} \left(\frac{\lambda_{td}}{\lambda^3}\right)^2,$$

$$x_s = 1.75 \left(\frac{m_t}{40\ \text{GeV}/c^2}\right)^2 \frac{\mathcal{B} f_{B_s}^2}{(150\ \text{MeV})^2} \left(\frac{\lambda_{ts}}{\lambda^2}\right)^2, \qquad (20)$$

where we have used the expectations in the Wolfenstein parametrization of the CKM matrix, which gives [27]

$$\lambda_{td} \leqslant \lambda^3 , \quad \lambda_{ts} \sim \lambda^2 \tag{21}$$

with $\lambda = \sin\theta_c \sim 0.23$. Thus the expectations in the standard model are

$$\chi_d \leqslant 10^{-2} , \quad 0.25 \leqslant \chi_s \leqslant 0.5 , \tag{22}$$

giving $\chi \leqslant 0.10$.

In table 3 we list the expectations for the dimuon ratio $R(\pm\pm/+-)$ for $m_t = 23$ GeV/c^2 and $m_t = 40$ GeV/c^2, $P_s = 0.16$ and $P_s = 0.20$. For $P_s = 0.20$, $\chi_s = 0.5$ and $m_t = 40$ GeV/c^2, we expect $R(\pm\pm/+-) = 0.38$, which is in good agreement with the UA1 measurements. Since the hypothesis of $B^0-\bar{B}^0$ mixing provides a plausible explanation for $R(\pm\pm/+-)$, one could extract χ from the UA1 data, getting

$$\chi > 0.043 , \quad (1.64\sigma) ,$$

$$\chi > 0.025 \quad (2\sigma) . \tag{23}$$

These numbers are to be compared with the limits from e^+e^- experiments

$$\text{from ARGUS [8]}, \ \chi_d < 0.11 \quad (90\% \text{ CL}) \tag{24a}$$

$$\text{from MARK II [7]}, \ \chi < 0.12 \quad (90\% \text{CL}). \tag{24b}$$

Apart from the ARGUS limit, which gives $r_d < 0.12$, both the UA1 and MARK II limits can be transcribed in terms of r_d and r_s only if one assumes P_d and P_s, as is obvious from eq. (14). Using $P_d = 0.4$, the ARGUS limit alone would give for the UA1 data

$$\chi < 0.044 \quad (90\% \text{ CL}) . \tag{25}$$

Comparing (23) and (25) it is easy to see that the *data alone* are themselves not enough to set a 90% CL lower bound on χ_s. At 68% CL, however, one gets

$$P_s \chi_s > 0.03 \quad (68\% \text{ CL}) , \tag{26}$$

which for $P_s = 0.20$ gives $r_s > 0.18$. The lower bounds from the UA1 data on r_d and r_s are shown in fig. 2 (curve f), where we also show the corresponding upper bounds from e^+e^- experiments (curves a–d) and expectations in the standard model (curve e).

In the *standard model*, however, one could get a 2σ lower bound on χ_s (or r_s) from the UA1 measurements. This can be obtained by neglecting χ_d, which is expected to be $O(10^{-2})$ in the standard model (eq. (22)). The resulting lower bound on χ (eq. (23)) now gives

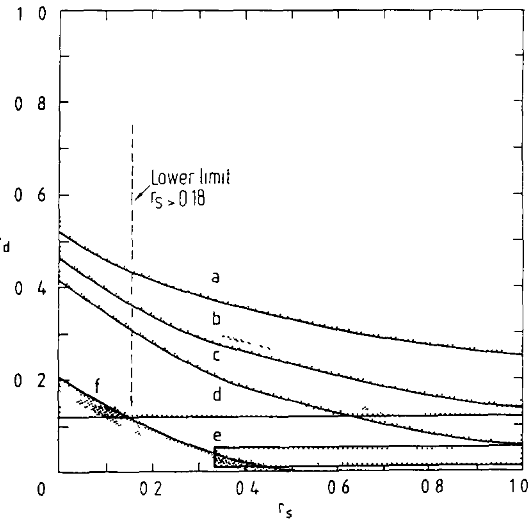

Fig. 2. Upper limits on the $B^0_d-\bar{B}^0_d$ mixing probability, r_d, and the $B^0_s-\bar{B}^0_s$ mixing probability, r_s, from e^+e^- experiments (curves a–d), the standard model prediction (curve e) and the lower limits on r_d and r_s from the UA1 dimuon ratio $R(\pm\pm/+-)$ (curve f). (a)–(c) MARK II limits [29], (a) $P_d = 0.35, P_s = 0.10$, (b) $P_d = 0.375, P_s = 0.15$, (c) $P_d = 0.40$, $P_s = 0.20$, (d) ARGUS limits from $\Upsilon(4s) \to B\bar{B}$ [8], (e) standard model estimates [19], (f) UA1 limits with $P_d = 0.4, P_s = 0.2$ [1]

$$P_s \chi_s > 0.025 \quad (2\sigma) , \tag{27}$$

which for $P_s = 0.20$ results in $r_s \geqslant 0.14$ (2σ). In fig. 3 we plot the bounds on the CKM matrix elements $|V_{td}|^{max}$ and $|V_{ts}|^{min}$ as functions of m_t, from the limits on r_d and r_s as explained above,

$$\text{for ARGUS,} \quad r_d < 0.12 \quad (90\% \text{ CL}) \tag{28a}$$

$$\text{for UA1 and SM,} \quad r_s > 0.14 \quad (2\sigma) . \tag{28b}$$

The shaded area reflects the uncertainty due to the bottom lifetime measurements. To have a numerical feeling, we quote the bounds taking $m_t = 40$ GeV/c^2,

$$|V_{td}| < 0.042 , \quad |V_{ts}| > 0.030 . \tag{29}$$

We emphasize that the UA1 lower bound on r_s makes it mandatory that the top quark exists, and within the standard model it provides the first direct evidence that the matrix element $|V_{ts}| \neq 0$. It is interesting to ask the question whether the bounds on $|V_{td}|$ and $|V_{ts}|$ obtained from r_d and r_s as shown in

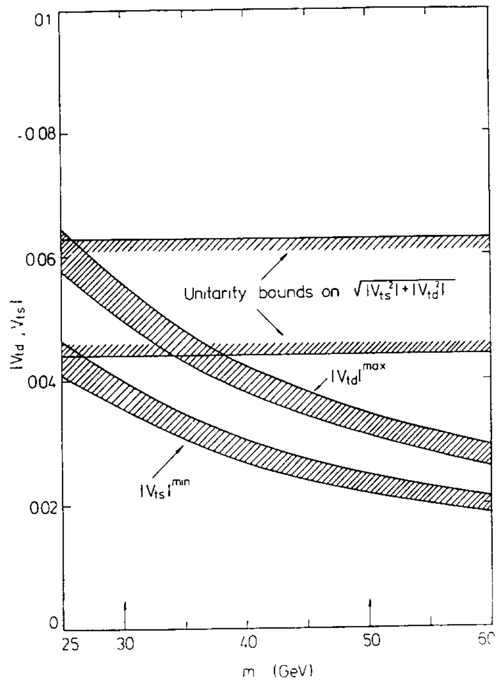

Fig. 3. Upper bounds on the CKM matrix element $|V_{td}|$ and the lower bond on $|V_{ts}|$ from the limits $r_d < 0.12$ (ARGUS) and $r_s > 0.14$ (UA1) as a function of the top mass, m_t. The bands for $|V_{td}|^{max}$ and $|V_{ts}|^{min}$ correspond to the $\pm 1\sigma$ allowed values of the bottom lifetime, $\tau_B = (1.11 \pm 0.14) \times 10^{-12}$ s. The (m_t independent) unitarity bounds on $(|V_{td}|^2 + |V_{ts}|^2)^{1/2}$ in the standard three family model are also shown.

fig. 3 are consistent with the expectations in the standard model. To that end we remark in the standard three-family model, one has the unitarity relation

$$|V_{td}|^2 + |V_{ts}|^2 = |V_{bc}|^2 + |V_{bu}|^2 \,. \tag{30}$$

Since τ_B essentially determines $|V_{bc}| = 0.05$ (+0.01/−0.006) [19] and $|V_{bu}|$ is bounded by $R < 0.12$ [28], giving $|V_{bu}| < 0.015$ [22,29], one has the unitarity bound (independent of m_t)

$$0.044 < (|V_{td}|^2 + |V_{ts}|^2)^{1/2} \leqslant 0.062 \,, \tag{31}$$

which is also shown in fig. 3. We remark that the bounds from B^0–$\bar{B}^0$ mixings (28) and the unitarity bounds (31) are compatible with each other for a rather large range of values of m_t. A possible conflict between a substantially higher value of r_s, a smaller value of m_t and the unitary bounds (31) though, cannot be excluded. Such a scenario would be a positive indication for new physics beyond the standard model. It is, therefore, extremely interesting to improve present measurements of r_d, r_s and m_t.

In conclusion, we have reported a calculation of the inclusive muon and dimuon data measured by the UA1 collaboration in the context of perturbative QCD. The data are well explained in inclusive rates and in a large number of distributions. The dimuon ratio $R(\pm\pm/+-)$, however, is a factor 1.8 too large in the data. The hypothesis of substantial B_s^0–$\bar{B}_s^0$ mixing explains quantitatively the measured ratio. The world data are found to be consistent with each other in terms of bounds on the mixing probabilities r_d and r_s, all of them are consistent with the standard model. At 2σ we determine $r_s > 0.14$. This gives a lower bound in the standard model on the matrix element $|V_{ts}|$, which for $m_t = 40$ GeV/c^2 is found to be greater than 0.030.

We would like to express our thanks to our colleagues at CERN and DESY for numerous discussions, in particular, K. Eggert, N. Ellis, M. Della Negra and C. Rubbia. One of us (BvE) would like to thank the theoretical physics group at DESY for its hospitality. All of us are grateful to the theoretical physics division at CERN for its generous support, where a good part of this work was done.

References

[1] UA1 Collab., G. Arnison et al., to be published, K. Eggert, New particles 1985, Conf. Proc. (University of Wisconsin, Madison, WI, 1985).
[2] See e.g., C. Caso, Proc. 1985 Intern. Symp. on Lepton and photon interactions at high energies (Kyoto, Japan, 1985), eds. M. Konuma and K. Takahashi, p. 488, and references quoted therein.
[3] A. Ali, B. Van Eijk and I. ten Have, CERN Report TH-4523/86 (1986).
[4] See e.g., L. Dilella and C. Rubbia, in. Proc. 1985 Intern. Symp. on Lepton and photon interactions at high energies (Kyoto, Japan, 1985), eds. M. Konuma and K. Takahashi.
[5] A. Ali and C. Jarlskog, Phys. Lett. B 114 (1984) 266.
[6] J. Ellis et al., Nucl. Phys. B 131 (1977) 285; A. Ali and Z.Z. Aydin, Nucl. Phys. B 148 (1979) 165.
[7] MARK II Collab., T. Schaad et al., Phys. Lett. B 160 (1985) 188.
[8] ARGUS Collab., H. Albrecht et al., contrib. paper XXIII Intern. Conf. on High energy physics (Berkeley, CA, 1986).

[9] N. Cabibbo, Phys. Rev. Lett. 10 (1963) 531;
M. Kobayashi and K. Maskawa, Prog Theor. Phys. 49 (1973) 652
[10] B.I. Combridge, Nucl. Phys. B 151 (1979) 429;
R. Horgan and M. Jacob, Nucl Phys. B 238 (1984) 221.
[11] Z. Kunszt and E. Pietarinen, Nucl. Phys. B 164 (1980) 45.
[12] G. Altarelli et al., Nucl. Phys. B 246 (1984) 12;
S.D. Ellis, R. Kleiss and W.J. Stirling, Phys. Lett. B 154 (1985) 435.
[13] R.K. Ellis, Fermilab Conf-86/35-T (1986).
[14] G Sterman and S Weinberg, Phys. Rev. Lett 39 (1977) 1436
[15] E Eichten et al., Rev. Mod. Phys. 56 (1984) 579
[16] UA Collab., G. Arnison et al , Phys Lett B 177 (1986) 244
[17] C. Peterson, D. Schlatter, I. Schmitt and P.M. Zerwas, Phys. Rev. D 27 (1983) 105.
[18] S Bethke, Z. Phys. C 29 (1985) 175.
[19] A Ali, in. Physics at LEP, CERN Report 86-02, Vol. 2 (CERN, Geneva, 1986) p 220.
[20] A. Ali, B. Van Eijk and E Pietarinen, EUROJET, a Monte Carlo event generator for hard partonic collisions, to be published;
see also B. Van Eijk, Proc. 5th Topical Workshop on Proton–antiproton collider physics (St. Vincent Aosta, Italy, 1985).
[21] See e.g. S. Komamiya, in: Proc. 1985 Intern. Symp. on Lepton and photon interactions at high energies (Kyoto, Japan, 1985), eds. M. Konuma and K. Takahashi.
[22] A.J. Buras, W. Slominski and H. Steger, Nucl. Phys. B 245 (1984) 369
[23] L.B. Okun, V.I Zacharov and B.M. Pontecorvo, Lett. Nuovo Cimento 13 (1975) 218,
A. Pais and S.B Treiman, Phys. Rev D 12 (1975) 244.
[24] M.A. Shifman and M V. Voloshin, ITEP Reports 86-54, 86-83 (1986), to be published.
[25] F Gilman and M Wise, Phys. Rev. D 21 (1980) 3150.
[26] M. Gilchrese, Proc. XXII Intern. Conf on High energy physics (Berkeley, CA, 1986).
[27] L. Wolfenstein, Phys. Rev. Lett 51 (1983) 1945.
[28] D. Kreinick, Proc Intern Symp on Production and decay of heavy flavours (Heidelberg, FRG, 1986).
[29] Particle Data Group, M. Aguilar-Benitez et al., Review of Particle Properties, Phys. Lett. B 170 (1986) 1.